0026-895X/88/040370-08$02.00/0

MOLECULAR PHARMACOLOGY, 33:370–377

Somatostatin Receptor Subtypes in the Clonal Anterior Pituitary Cell Lines AtT-20 and GH3

KYRIAKI THERMOS and TERRY REISINE

Department of Pharmacology, University of Pennsylvania School of Medicine, Philadelphia Pennsylvania 19104

Received September 21, 1987; Accepted January 29, 1988

SUMMARY

The functional and biochemical characteristics of somatostatin (somatotropin release-inhibiting factor) (SRIF) receptor subtypes were examined in the clonal pituitary cell lines AtT-20 and GH3. SRIF inhibits evoked calcium influx into each of these cell lines. The rank order of potencies of structural analogues of SRIF to inhibit calcium influx into GH3 versus AtT-20 cells was different. Inhibitory actions of SRIF on calcium influx densensitized in AtT-20 cells but not GH3 cells. The biochemical properties of the SRIF receptor subtypes in AtT-20 and GH3 cells were assessed by photoaffinity labeling of each receptor with the nonreducible SRIF analogue [^{125}I]CGP 23996 and the photocrosslinking agent *n*-hydroxysuccinimidyl-4-azidobenzoate. The covalently labeled receptors in both cell lines had the same size, 55 ± 5 kDa, as assessed by sodium dodecyl sulfate-polyacrylamide gel electrophoresis. The covalent binding of [^{125}I]CGP-23996 to GH3 and AtT-20 cell membranes was blocked by 1 μM SRIF, somatostatin 28, Trp8-SRIF and was GTP sensitive. Analysis of the labeled receptors in GH3 and AtT-20 cell membranes by two-dimensional polyacrylamide gel electrophoresis indicated that they were of similar charge (pI = 6–6.5) and that they comigrate when applied together. Proteolysis of the GH3 and AtT-20 cell SRIF receptors with *Staphyloccus aureus* V-8 and thermolysin revealed similar peptide maps. Pretreatment of AtT-20 cells with different stable SRIF analogues abolished the subsequent equilibrium or covalent labeling of the SRIF receptor with [^{125}I]CGP-23996. Similar treatment of GH3 cells did not reduce the covalent labeling of the SRIF receptor by [^{125}I]CGP 23996. These studies indicate that the functional characteristics of SRIF receptors in GH3 and AtT-20 cells are different. However, clear differences in the biochemical properties of these receptor subtypes were not observed. Subtle variations in the structure of the SRIF receptors may therefore be responsible for the functional differences.

The neuropeptide SRIF exerts diverse physiological actions in the central nervous system as well as in peripheral organs (for review see Ref. 1). Receptors for SRIF have been characterized in different tissues including the cerebral cortex, anterior pituitary, and pancreas (2–7). In these tissues, SRIF receptors exhibit high affinity for SRIF analogues and appear as a single population of noninteracting sites. The urinary nature of the SRIF receptor is supported by the studies of Sakamoto *et al.* (7) who observed that the high affinity SRIF ligand [^{125}I] Tyr1-SRIF could be photocrosslinked to a single protein in pancreatic acinar membranes.

A number of investigators, however, have suggested that subtypes of SRIF receptors exist. Srikant and Patel (2) and Reubi (8) showed that SRIF and the prohormone somatostatin 28 had a reverse rank order of potency in blocking [^{125}I]Tyr11-SRIF binding in rat brain cerebral cortical and pituitary membranes. Tran *et al.* (9) observed that two potent SRIF analogues, SMS 201-995 and cyclo(Ala-Cys-Phe-DTrp-Lys-Thr-Cys) inhibited [^{125}I]Tyr11-SRIF binding to brain tissue in a biphasic manner. These authors proposed the presence of high and low affinity SRIF receptors in brain. Brown *et al.* (10) and Mandarino *et al.* (11) also observed a reverse order of potency of SRIF and somatostatin 28 in blocking *in vivo* insulin and glucagon release, implying distinct SRIF receptor subtypes in pancreas. This hypothesis was supported by Srikant and Patel (6), who showed that [^{125}I]Tyr11-SRIF could be photocrosslinked to three proteins in pancreatic membranes.

SRIF receptor subtypes may also exist in the anterior pituitary. Two tumor cell lines have been used extensively to characterize pituitary SRIF receptors. AtT-20 cells synthesize proopiomelanocortin and secrete adrenocorticotropin (12). GH3 cells and its subclone, GH4C1, release prolactin and growth hormone (13). SRIF inhibits hormone release from both of these cell lines through an activation of specific receptors (12, 13). SRIF and somatostatin 28 have a reverse rank order of potency to block hormone release and cAMP formation in

This work was supported by National Institutes of Health Grants DK37404 and GM34781, and by an American Heart Association grant-in-aid.

ABBREVIATIONS: SRIF, somatostatin (somatotropin release-inhibiting factor); Quin 2AM, the acetomethoxy methylester of Quin 2; Quin 2, 2-{[2-bis-(carboxymethyl)-amino-5-methylphenoxy]-methyl}-6-methoxy-8-bis-carboxymethyl-aminoquinoline; CRF, corticotropin-releasing factor; DMEM, Dulbecco's modified Eagle's medium; PBS, phosphate-buffered saline; BSA, bovine serum albumin; EGTA, ethylene glycol bis(β-aminoethyl ether)-*N*, *N*, *N′*, *N′*-tetraacetic acid; HSAB, *n*-hydroxysuccinimidyl-4-azidobenzoate SDS, sodium dodecyl sulfate; PAGE, polyacrylamide gel electrophoresis.

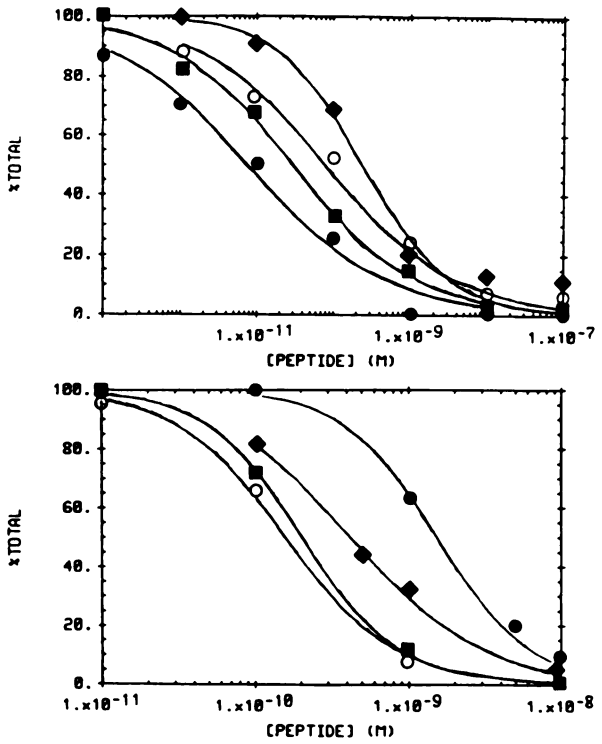

Fig. 1. SRIF analogues inhibit forskolin-stimulated calcium influx into AtT-20 calls and GH3 cells. AtT-20 cells (*top*) and GH3 cells (*bottom*) were stimulated with forskolin (10 μM). The ability of different concentrations of SRIF (○), somatostatin 28 (●), Trp8-SRIF (■), and Tyr11 SRIF (♦) to inhibit the calcium influx induced by forskolin was tested. Experiments were performed as described under Experimental Procedures. The inhibition curves were generated using the NEWFITSITES program available in the PROPHET system. The curves are computer drawn and represent the means of six to eight different experiments for each peptide. The mean ± standard error IC_{50} values generated from these curves are presented in Table 1. It should be noted that the *x* axes in the *top* and *bottom* panels are different.

TABLE 1

Inhibition of forskolin-stimulated calcium influx into AtT-20 and GH3 cells

Values represent the mean ± standard error IC_{50} values of six to eight different determinations for SRIF, somatostatin 28 (SS28), Trp8-SRIF(Trp8) and Tyr11-SRIF (Tyr11) inhibiting forskolin-stimulated calcium influx into AtT-20 cells and GH3 cells. IC_{50} values were generated using the PROPHET program. The curves were best fitted for a single site.

	IC_{50} Value			
	SRIF	SS28	Trp8	Tyr11
AtT-20	64 ± 13	8 ± 3	30 ± 11	237 ± 19
GH3	150 ± 27	1507 ± 420	200 ± 14	412 ± 40

these cells, and these peptides have different orders of potencies to inhibit [^{125}I]Tyr11-SRIF or [^{125}I]CGP 23996 (a nonreducible SRIF analogue) binding to GH3 and AtT-20 cell membranes (13–15).

In the present study, the functional characteristics of SRIF receptors in these cell lines are further distinguished. SRIF analogues have a different rank order of potency to block calcium influx in these two cell lines, and the responses of GH3 and AtT-20 cells to SRIF are differentially regulated. To determine whether the contrasting functional characteristics of these receptor subtypes are due to variations in their biochemical properties, the SRIF receptors from AtT-20 and GH3 were photoaffinity labeled with the SRIF analogue, [^{125}I]CGP 23996. The covalently labeled protein in each cell had the same size and charge, and exhibited similar peptide maps following proteolytic digestion. These studies suggest that the functional differences in these SRIF receptor subtypes may be due to subtle structural variations in the receptor or its neighboring membrane environment.

Experimental Procedures

Materials. Quin 2AM, forskolin, and ionomycin were purchased from Calbiochem-Behring (San Diego, CA). CRF, SRIF, Trp8-SRIF, Tyr11-SRIF, and somatostatin 28 were obtained from Peninsula Laboratories (San Carlos, CA). SMS 201-995 was obtained from Sandoz (Basel, Switzerland). DMEM and RPMI-1640 (with L-glutamine) were obtained from the cell center at the University of Pennsylvania (Philadelphia, PA). *Staphyloccus aureus* V-8 was from ICN (Lisle, IL) and thermolysin from Calbiochem. Molecular weight standards for gel electrophoresis were obtained from Bethesda Research Laboratories (Bethesda, MD) and all other materials for gel electrophoresis were from Bio-Rad (Rockville Center, NY). Isoelectric focusing standards were obtained from U.S. Biochemicals (Cleveland, OH) and the ampholytes were from LKB (Gaithersburg, MD). Bacitracin and all other biochemicals were obtained from Sigma Chemical Co. (St. Louis, MO). SRIF and its analogs were prepared as stock solutions (100 μM) in acidified PBS (pH 1).

Cell culture techniques. Mouse AtT-20/D16-16 tumor cells (subcloned by Dr. S. Sabol, National Institutes of Health) were grown and subcultured in DMEM with 10% fetal calf serum as previously described (14). Cells were plated in 75-cm^2 culture flasks at an initial density of one million cells/flask and were used 4–5 days after subculturing (60–80% confluency).

Quin 2 Fluorescence studies. The procedures for the Quin 2 studies are as described previously (15). Briefly, the cells were washed twice by resuspension/centrifugation (500 × *g*, 5 min) in 10 ml of DMEM supplemented with 0.25% BSA. The cells were resuspended in 10 ml of DMEM/BSA and incubated with 50 μM (final concentration) of the acetomethoxy methylester of Quin 2 (Quin 2AM) for 15 min at 37° in a shaking water bath.

A 1-ml aliquot of the loaded cells was added to 10 ml of HBSS containing 0.02% (w/v) BSA at 37°. This sample was centrifuged, the supernatant was discarded, and the cells were resuspended in 2 ml of Hanks' balanced salts solution/DMEM. This suspension was then transferred to a quartz fluorimeter cuvette and the cell fluorescence was determined in a temperature-controlled (at 37°) fluorescence spectrophotometer. The excitation wavelength was 339 nm (slit width 5 nm) and the emission wavelength was 492 nm (slit width 10 nm).

The cell suspensions were then challenged by test agents (CRF, forskolin, or SRIF analogues). The fluorescence signal was continuously measured for at least 20 min following the challenge with any of the agents. At the end of each experiment, 4 μg of ionomycin were added to the cells (to equilibrate intracellular calcium levels with the calcium in the extracellular medium), and the resulting fluorescence signal, which corresponds to a calcium concentration of 1 mM, was designated maximal fluorescence (F_{max}). The cells were then sonicated with a Branson Sonicator (10 W, 5 sec). Enough EGTA was added to reduce the concentration of free calcium below 1 nM. The resulting fluorescence signal was designated minimal fluorescence (F_{min}). These values of F_{max} and F_{min} were used to determine the concentration of free calcium corresponding to the experimental fluorescence signals by the equation of Tsien *et al.* (16).

Membrane preparation. AtT-20 and GH3 cells were harvested with 50 mM Tris-HCl (pH 7.4) and centrifuged for 15 min at 20,000 × *g*. The pellet was homogenized in a Polytron (Brinkmann, setting 5, 10 sec) in Tris buffer containing 20 μg/ml bacitracin, and this membrane preparation was used for the binding and photocrosslinking studies. The anterior pituitary was removed from Sprague-Dawley rats following decapitation and homogenized in a Polytron in Tris-HCl buffer,

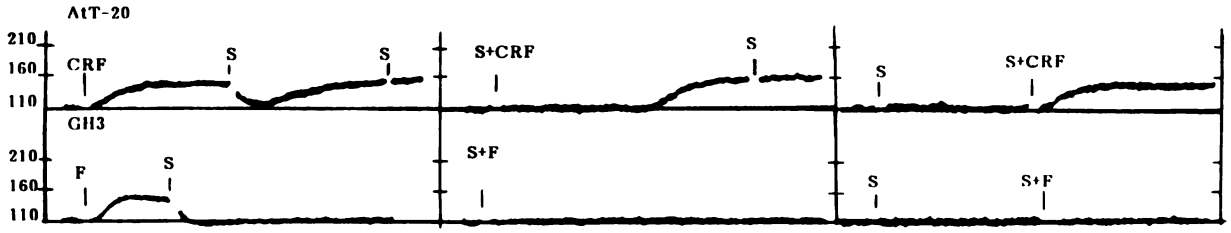

Fig. 2. Comparison of the effects of SRIF pretreatment on AtT-20 and GH3 cells. AtT-20 cells (*top*) were stimulated by CRF (100 nM) alone or in combination with SRIF (*S*) (100 nM). The effect of SRIF pretreatment on the subsequent ability of SRIF to block CRF-stimulated calcium influx was measured. GH3 cells (*bottom*) were stimulated by forskolin (10 μM) (*F*) either alone or in combination with SRIF (100 nM). The same manipulations as performed on AtT-20 cells were initiated on the GH3 cells. Once the drugs (CRF, forskolin, SRIF, or their combination) are applied to the cells (indicated by *vertical lines*), they remain in contact with the cells throughout the duration of the experiments. The levels of intracellular calcium are presented to the *left* of the traces. These are representative traces of individual experiments repeated four to five different times. A time scale (1 min) is presented as a *bar*.

pH 7.4. Membranes were prepared by centrifugation at 20,000 × *g* for 15 min at 4°.

Radioligand binding and photocrosslinking assay. SRIF receptor binding assays were performed as previously described (4, 15) by incubating AtT-20 and GH3 cell membranes in Tris/bacitracin buffer with 1 nM [^{125}I]CGP 23996 (specific activity 1000 Ci/mmol) for 60 min at 25°. Nonspecific binding was the binding remaining in the presence of 1 μM Trp8-SRIF. Receptor specific [^{125}I]CGP 23996 binding accounted for 70–80% of total binding. The binding reaction was terminated by vacuum filtration over Whatman GF/C glass fiber filters. The filters were washed with 15 ml of Tris-HCl buffer. The bound radioactivity was then analyzed in a gamma counter (80% efficiency). For the photocrosslinking experiments the incubation mixture was centrifuged twice at 35,000 × *g* for 5 min at 4°. The pellet was resuspended in PBS, and the photoreactive cross-linking reagent HSAB (freshly dissolved in dimethyl sulfoxide) was added immediately at a final concentration of 0.1 mM. The mixture was exposed to UV light (Ace Hanova 450-W lamp, from a distance of 15 cm) for 15 min on ice and under constant stirring. The photocrosslinked membranes were then centrifuged at 35,000 × *g* for 5 min and the pellet was solubilized in either SDS-sample buffer or isoelectrofocusing buffer (9.5 M urea, 2% Nonidet P-40, 5% 2-mercaptoethanol, 2% LKB ampholytes, pH 3.5–10).

SDS-polyacrylamide gel electrophoresis. Gel electrophoresis was performed according to the method of Laemmli (17) using 1.5-mm-thick slab gels containing 10 or 15% acrylamide. Following electrophoresis the gels were fixed in 3% trichloroacetic acid for 2 hr and dried using a Bio-Rad model 483 slab dryer. Autoradiograms were obtained from the dried gels after exposure to Kodak XAR-5 film with a DuPont Cronex Lightening Plus intensifying screen at −70°.

Two-dimensional PAGE. Two-dimensional PAGE was performed according to the procedure of O'Farrell (18). The isoelectrofocusing gels contained 2% total ampholytes, pH 3.5–10, 4–6, 5–7, in the proportions 2:1:1. Isoelectric focusing was run at 500 V for 16 hr. The second dimension was run as described previously for one-dimensional PAGE on 10% acrylamide.

Peptide Mapping. Limited proteolysis was performed according to the procedure of Cleveland *et al.* (19) with minor modifications. Briefly, following photocrosslinking, the mixtures were centrifuged at 35,000 × *g* for 5 min at 4°. The pellets were solubilized in 2 × SDS-sample buffer and proteolysis was initiated upon addition of *S. aureus* V-8 (2.5 μg) or thermolysin (25 μg), dissolved in 20 mM Tris-HCl, pH 6.8. The samples were then incubated at 25° for different time periods and then proteolysis was stopped by immersing the samples in boiling water for 2 min. The samples were then electrophoresed on one-dimensional PAGE (15% acrylamide gel) overnight at 60 V.

SRIF inhibition curves. The potency of SRIF analogues in blocking forskolin-stimulated calcium influx in AtT-20 cells and GH3 cells (see Fig. 1 under Results) was assessed in the following manner. Forskolin was applied to the cells with or without the SRIF analogue. The percentage reduction of intracellular calcium (compared to the maximal stimulation induced by forskolin) was calculated for each of the different concentrations of the SRIF analogues. These data were used to generate the inhibition curves. IC_{50} values were obtained from curve fitting by nonlinear least squares regression analysis. The analysis was performed by the mathematical modeling program NEWFIT-SITES (20) available on the National Institutes of Health-sponsored PROPHET system.

Results

Cytosolic calcium. Intracellular calcium levels were measured using the fluorescence probe Quin 2. Free cytosolic calcium levels are increased in AtT-20 and GH3 cells by forskolin (15, 21). This rise in cytosolic calcium is due to an increase in calcium influx (22). High concentrations of SRIF have been shown to block forskolin-stimulated calcium influx into AtT-20 and GH3 cells (15, 21). Somatostatin 28 is significantly more potent than SRIF in blocking forskolin-stimulated calcium influx into AtT-20 cells (Fig. 1, Table 1). In contrast, SRIF is more potent than its prohormone in preventing the calcium influx evoked by forskolin in GH3 cells (Fig. 1, Table 1). The rank order of potency of SRIF analogues to inhibit calcium influx into AtT-20 and GH3 cells is different.

In AtT-20 cells stimulated by CRF (Fig. 2) or forskolin (not shown), SRIF immediately reduced cystolic calcium concentrations to basal levels (Fig. 2). Within 3 min after the application of SRIF, cytosolic calcium levels increased. Five min after the addition of SRIF, cytosolic calcium levels were the same as that seen with CRF or forskolin alone. Reapplication of SRIF did not reduce intracellular calcium levels.

Simultaneous exposure of AtT-20 cells to SRIF and CRF resulted in no change in basal cytosolic calcium levels for 5 min (Fig. 2). Afterward, cytosolic calcium concentrations increased to the same level as that seen with CRF alone despite the continued presence of SRIF. Reapplication of SRIF did not

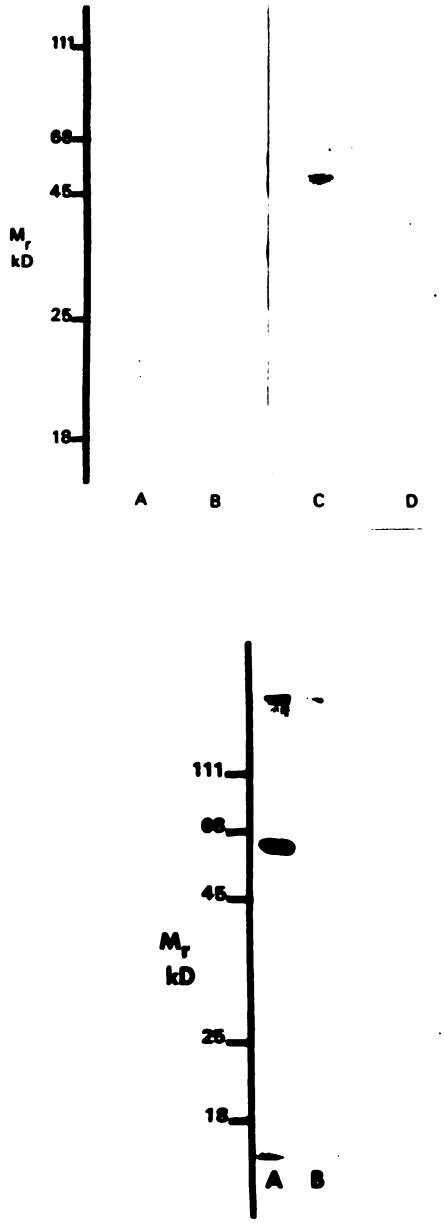

Fig. 3. Photoaffinity labeling of SRIF receptors in AtT-20 cells, GH3 cells, and rat anterior pituitary with [^{125}I]CGP 23996. *Top.* Membranes prepared from AtT-20 (lanes *A* and *B*) and GH3 cells (lanes *C* and *D*) (derived from 5 million cells) were incubated with [^{125}I]CGP 23996 (1 nM) for 60 min at 25° in the presence (lanes *B* and *D*) or absence (lanes *A* and *C*) of unlabeled Trp8-SRIF (1 μM). Subsequently, the membranes were photocrosslinked in the presence of HSAB (0.1 mM) and the samples were electrophoresed on 10% acrylamide gels. The gels were dried and autoradiography was performed as described under Experimental Procedures. These representative experiments were repeated three different times with similar results. *Bottom.* Membranes from the rat anterior pituitary (two anterior pituitaries obtained from male Sprague-Dawley rats, 250 g) were incubated with [^{125}I]CGP 23996 in the presence (lane *B*) and absence (lane *A*) of unlabeled Trp8-SRIF (1 μM). The membranes were subjected to photoaffinity labeling with [^{125}I]CGP 23996 and SDS-PAGE as described under Experimental Procedures. These experiments were repeated twice with similar results.

lower cytosolic calcium levels. Prior exposure of AtT-20 cells to SRIF abolished the ability of the peptides to inhibit CRF-stimulated calcium influx. Similar results were obtained using forskolin as the stimulant of calcium influx (not shown).

In contrast to the SRIF desensitization observed in AtT-20 cells, SRIF induced a sustained inhibition of forskolin-stimulated calcium influx into GH3 cells (Fig. 2). Similar results were obtained when calcium influx was evoked by the hormone vasoactive intestinal peptide, an activator of adenylate cyclase (not shown).

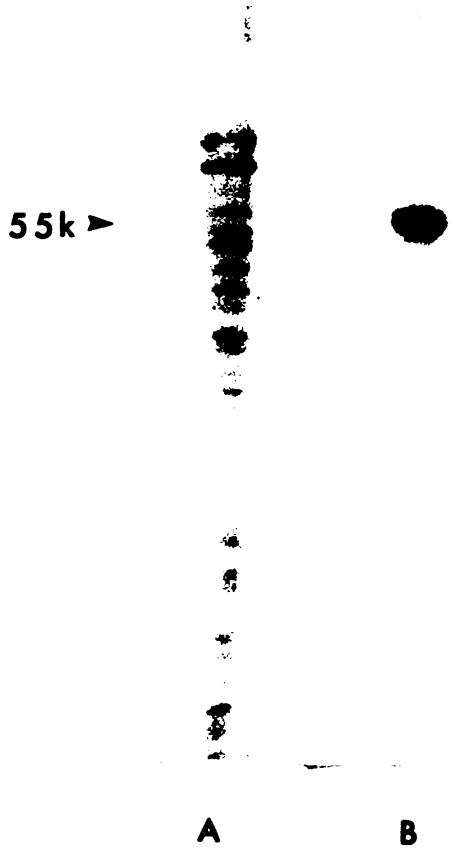

Fig. 4. Coomassie blue stain pattern and autoradiography of proteins labeled with [^{125}I]CGP 23996 in AtT-20 cell membranes. Membranes from AtT-20 cells (5 million cells) were prepared, photocrosslinked with [^{125}I]CGP 23996, and separated on a 10% gel as described under Experimental Procedures. The gel was stained with Coomassie blue and subsequently dried and exposed to Kodak X-OMAT film. The protein stain is presented in lane *A* and the autoradiogram of the [^{125}I]CGP 23996 labeling is in lane *B*.

Photocrosslinking of [^{125}I]CGP 23996 to SRIF receptors. To determine whether functional differences of the SRIF receptors in GH3 and AtT-20 cells were due to biochemical variations in the receptors, the SRIF receptors in both cell lines were photoaffinity labeled to the SRIF analogue [^{125}I]CGP 23996. The labeled proteins were analyzed by SDS-PAGE. Previous studies have shown that [^{125}I]CGP 23996 specifically labels the SRIF receptor in a variety of cells and tissues (4, 15). This peptidase-resistant SRIF analogue was bound to membranes prepared from AtT-20 and GH3 cells, and subsequently photocrosslinked to the heterobifunctional reagent HSAB using the procedure previously described by Sakamoto *et al.* (7).

[^{125}I]CGP 23996 bound covalently to a single component with an apparent molecular mass of 55 ± 5 kDa in both AtT-20 and GH3 cells as well as rat anterior pituitary (Fig. 3). Despite the presence of numerous proteins in the AtT-20 cell homogenates (as assessed by Coomassie blue staining), only one protein band was labeled by [^{125}I]CGP 23996 (Fig. 4). The labeling of this component by [^{125}I]CGP 23996 in AtT-20 cells, GH3 cells, and

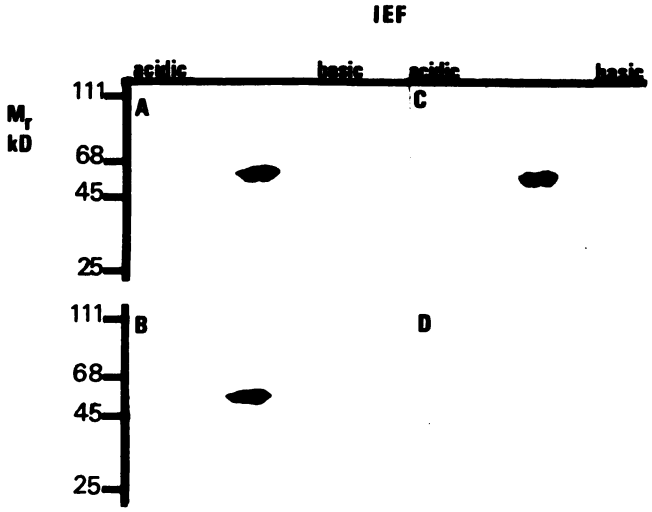

Fig. 5. Two-dimensional analysis of [^{125}I]CGP 23996-labeled proteins in AtT-20 and GH3 cells. Membranes from AtT-20 (A) and GH3 (B) cells (5 million cell each) were photoaffinity labeled with [^{125}I]CGP 23996 and the proteins were separated on two-dimensional SDS-PAGE as described under Experimental Procedures. A mixture of photolabeled AtT-20 and GH3 membranes in the absence (C) and presence (D) of Trp8-SRIF (1 uM) was electrophoresed as one sample.

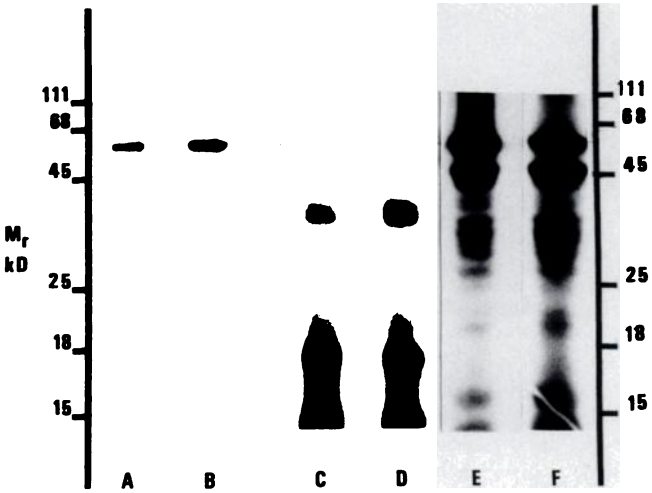

Fig. 6. Limited proteolysis of the radiolabeled SRIF receptor in AtT-20 and GH3 cells by thermolysin and *S. aureus* V-8. Membranes from AtT-20 (lanes *A*, *C*, and *E*) and GH3 (lanes *B*, *D*, and *F*) cells (5 million each) were photocrosslinked with [^{125}I]CGP 23996 and then treated with 2 × SDS sample buffer and either PBS alone (control, *A* and *B*) or thermolysin (25 μg; *C* and *D*) or *S. aureus* V-8 (2.5 μg; *E* and *F*). The samples containing thermolysin and *S. aureus* V-8 were incubated for 1 hr and 15 min, respectively, at 25° and then electrophoresed overnight at 60 V on 15% acrylamide gels.

rat anterior pituitary was completely abolished in the presence of Trp8-SRIF (Fig. 3), SRIF, and somatostatin 28 but not the inactive 1-14 fragment of somatostatin 28. Previous studies (15) have shown that the equilibrium binding of [^{125}I]CGP 23996 to AtT-20 cell membranes is not affected by other biologically active peptides such as vasopressin, cholecystokinin, or CRF. The stable guanine nucleotide analogue GppNHp (100 μM) also inhibited the photoincorporation of [^{125}I]CGP 23996 in AtT-20 and GH3 cells by 50 and 80%, respectively (data not shown).

To determine whether the 55-kDa band labeled with [^{125}I]CGP 23996 in AtT-20 and GH3 cells represents a single protein, the photocrosslinked material was separated on two-dimensional PAGE. This technique characterizes proteins according to their molecular mass as well as their charge (pI value). [^{125}I]CGP-23996 labels a single component in both AtT-20 and GH3 cells with very similar pI values, 6–6.5 (Figure 5, A and B). When the photocrosslinked material of AtT-20 and GH3 cells were mixed as one sample and run on two-dimensional PAGE, comigration of the labeled spots was observed (Fig. 5C). No labeling in the mixture (Fig. 5D) or for each tissue separately (not shown) was observed in the presence of excess Trp8-SRIF (1 μM).

Peptide mapping. To further investigate the biochemical properties of the SRIF receptors in AtT-20 and GH3 cells, the photocrosslinked receptors of both cells were subjected to limited proteolysis. Treatment of covalently labeled SRIF receptors from AtT-20 and GH3 cell membranes with *S. aureus* V-8 or thermolysin resulted in the appearance of similar peptide maps (Fig. 6).

Selective loss of [^{125}I]CGP 23996 binding to AtT-20 cell membranes following SRIF pretreatment. As shown in the studies above, SRIF responses in AtT-20 cells desensitized. This desensitization may be due to a modification of the SRIF receptor. Exposure of AtT-20 cells for 3 hr to either somatostatin 28 or the peptidase-resistant analogue of SRIF, SMS 201-995, resulted in a greater than 85% reduction of the equilibrium binding of [^{125}I]CGP 23996 binding to AtT-20 cell membranes (Fig. 7). The loss of [^{125}I]CGP-23996 binding was dependent on the concentration of somatostatin 28 in the pretreatment medium (Fig. 7). Decreases in [^{125}I]CGP 23996 binding were not observed in cells pretreated with 1 nM somatostatin 28 (Fig. 7). This concentration of somatostatin 28 completely inhibits calcium influx (Fig. 1), cAMP formation, and ACTH release (14). Therefore, 1 nM somatostatin 28 would be expected to fully occupy the SRIF receptors in AtT-20 cells. Thus, the decreases in [^{125}I]CGP 23996 binding following treatment with 10 nM and 100 nM concentrations of somatostatin 28 are probably not the result of a tight binding of the unlabeled peptides to the receptor but more likely reflect either a downregulation of the receptor or its sequestration.

SRIF pretreatment also reduced [^{125}I]CGP 23996 binding (Fig. 7). Exposure of AtT-20 cells for 2 hr with Trp8-SRIF abolished the subsequent ability of [^{125}I]CGP 23996 to be photocrosslinked to the SRIF receptor (Fig. 8). Pretreatment for as little as 5 min with Trp8-SRIF greatly reduced the ability of [^{125}I]CGP 23996 to covalently label the AtT-20 cell SRIF receptor (Table 2). In contrast to the findings in AtT-20 cells, 2–12 hr of Trp8-SRIF pretreatment of GH3 cells did not reduce the subsequent covalent labeling of the SRIF receptor with [^{125}I]CGP 23996 (Fig. 8, Table 2).

Discussion

Pharmacological studies have shown that functionally distinct SRIF receptor subtypes exist in brain and pancreas (2, 3, 8–11). Controversy exists whether physically different receptor subtypes mediate the actions of SRIF. Srikant and Patel (6) reported that [^{125}I]Tyr11-SRIF could be photocrosslinked to at least three different sized protein bands in pancreatic acinar membranes. Using similar procedures, Sakamoto *et al.* (7) observed that only one protein band, as assessed by SDS-PAGE, was photocrosslinked with [^{125}I]Tyr1-SRIF in this same

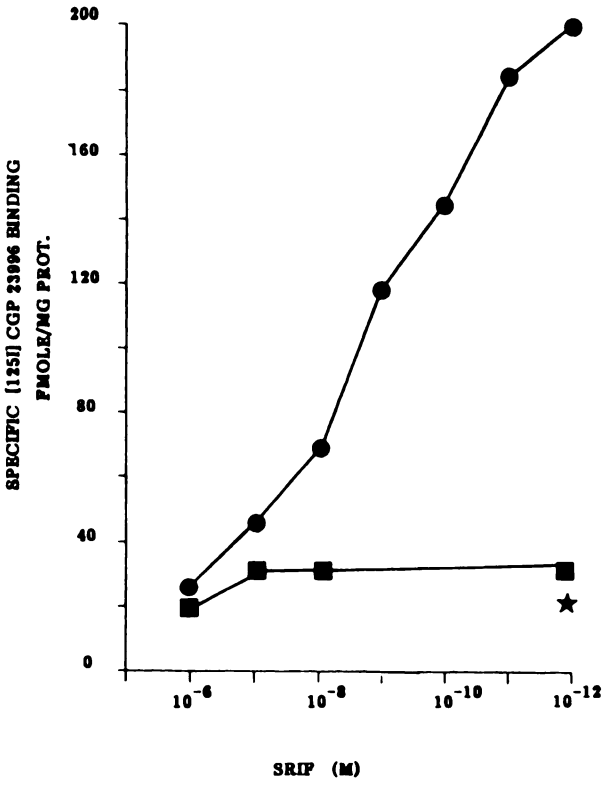

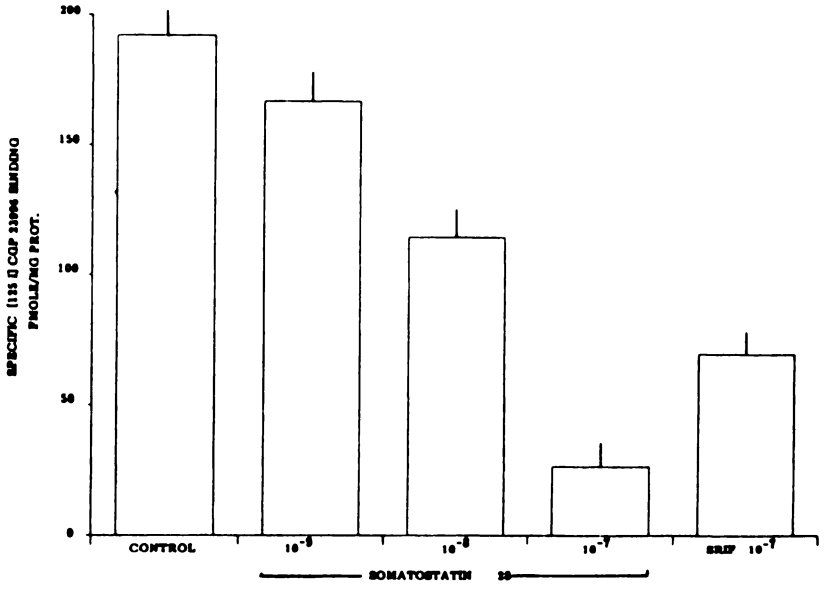

Fig. 7. Desensitization of SRIF receptors in AtT-20 cells. AtT-20 cells were treated for 3 hr with medium containing SMS 201-995 (100 nM) (★), somatostatin 28 (100 nM) (■), or control medium (●). The binding of [^{125}I]CGP 23996 (1 nM), under equilibrium condition, to membranes of the control and treated cells was performed as described under Experimental Procedures. The ability of different concentrations of SRIF to inhibit binding to each group was assessed (*top*). Specific binding was defined as the amount of [^{125}I]CGP 23996 binding displaced by 5 μM Trp8-SRIF. The IC_{50} value for SRIF inhibition of [^{125}I]CGP 23996 binding to control membranes was 1.0 ± 0.3 nM. Because of the low levels of specific [^{125}I]CGP 23996 binding in the somatostatin 28-treated membranes, it was not possible to generate an accurate IC_{50} value for SRIF inhibition. The effect of pretreating AtT-20 cells for 3 hr with different concentrations of somatostatin 28 on specific [^{125}I]CGP 23996 binding is presented in the *lower panel*. The effect of pretreating AtT-20 cells with SRIF (100 nM) for 3 hr on specific [^{125}I]CGP 23996 binding is also presented. These are the results of representative experiments repeated three other times with similar outcomes.

tissue. No explanation for these different findings is presently available.

To examine further whether biochemical variations exist between the SRIF receptor subtypes, the SRIF receptor in two homogeneous tumor cell lines of the anterior pituitary, GH3 and AtT-20, were characterized. These cell lines have served as model systems for the study of somatotrophs and corticotrophs, respectively (12, 13). Ligand binding experiments employing [^{125}I]Tyr11-SRIF have indicated that only a single population of SRIF receptors is present in GH3 cells having higher affinity for SRIF than somatostatin 28 (13). In the present study, SRIF is shown to be more potent than its prohormone in blocking forskolin-stimulated calcium influx into GH3 cells. The greater selectivity for SRIF over somatostatin 28 is also exhibited by SRIF receptors in brain and pancreatic α cells (2, 10, 11). In contrast, the SRIF receptor in AtT-20 cells have greater affinity for somatostatin 28 than SRIF. Somatostatin 28 is more potent than SRIF in blocking forskolin-stimulated calcium influx,

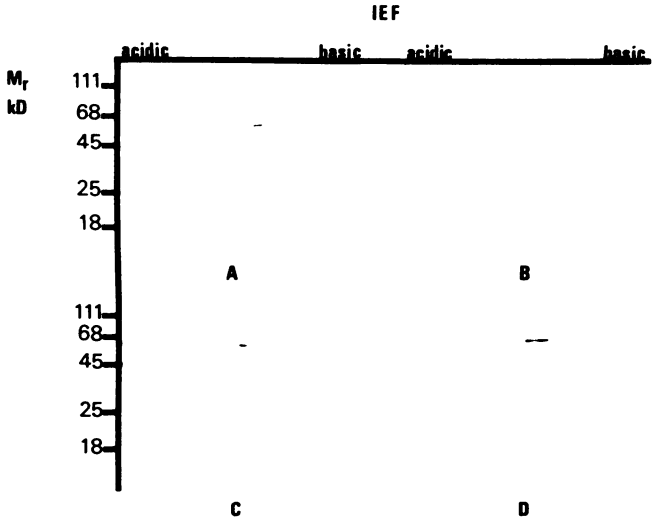

Fig. 8. Effect of Trp8-SRIF pretreatment on [^{125}I]CGP 23996 Photocrosslinking to SRIF receptors in AtT-20 and GH3 cells. AtT-20 and GH3 cells (5 million cells each) were treated with Trp8-SRIF (1 μM) for 2 hr. Immediately afterwards the cells were washed with PBS, membranes were prepared and photolabeled with [^{125}I]CGP 23996, and the proteins were separated by two-dimensional gel electrophoresis. A and B represent control and Trp8-SRIF-treated AtT-20 cells, respectively. C and D represent control and Trp8-SRIF-treated GH3 cells, respectively.

TABLE 2

Effect of Trp8-SRIF pretreatment on the ability of [^{125}I]CGP 23996 to label AtT-20 and GH3 cells

AtT-20 and GH3 cells were pretreated with Trp8-SRIF (1 μM) for varying periods. Control and treated cells were then washed twice with PBS, and the SRIF receptors in each tissue was photocrosslinked with [^{125}I]CGP 23996 as described under Experimental Procedures. The covalently labeled receptor was analyzed by two-dimensional PAGE as illustrated in Fig. 6. After autoradiography, the region of the dried gel of the untreated control AtT-20 and GH3 cells containing the labeled protein was cut out and the radioactivity assessed in a gamma counter. The corresponding region in the gels in which the treated membranes were analyzed was also excised and counted. The cpm represent corrected values (subtraction of cpm found in blank areas of the dried gel). In the AtT-20 cell study, the pretreatment abolished the labeling of the SRIF receptor. As a result, the autoradiograms did not reveal a radioactive spot. Therefore, we excised a region corresponding to the same size and pI value determined for the labeling in the control. These experiments were repeated one other time.

	AtT-20	GH3
	cpm	
Control	235	1127
SRIF pretreatment time (min)		
5	13	
15	8	
30	0	
60	0	
120	8	1224
720	59	1401

cAMP formation, and ACTH release (14). The SRIF receptors present in pancreatic β cells involved in the inhibition of insulin secretion have a similar selectivity for somatostatin 28 (10, 11).

In addition to these differences in pharmacological specificity, the SRIF receptors in GH3 and AtT-20 cells are differentially regulated. Brief periods of pretreatment of AtT-20 cells with SRIF are sufficient to desensitize the SRIF receptors. In contrast, the SRIF receptors in GH3 cells are much more resistant to desensitization. This is further suggested by the studies of Smith *et al.* (23), who observed that at least 12 hr of continuous exposure of anterior pituitary cells to SRIF were required to diminish the ability of this peptide to inhibit growth hormone and prolactin release. Few other cell types have been examined for SRIF desensitization. Marki *et al.* (24) reported that multiple subcutaneous injections of SRIF to rats gradually reduced the responsiveness of pancreatic β-cells to the inhibitory actions of SRIF on insulin release. In the same animals, the inhibition by SRIF of glucagon secretion from pancreatic α cells was maintained, further suggesting that the SRIF receptor subtypes can be differentially regulated.

Thus, the question arises whether the differences in functional characteristics of SRIF receptor subtypes could be due to biochemical variations in the SRIF receptor molecule. The SRIF receptors in GH3 and AtT-20 cells were photoaffinity labeled by the SRIF analogue [^{125}I]CGP 23996 in order to investigate their physical properties. [^{125}I]CGP 23996 covalently labeled similar sized proteins in AtT-20 and GH3 cells. The labeling was selectively blocked by SRIF and various biologically active SRIF analogues. [^{125}I]CGP 23996 was also able to covalently label a 55-kDa protein in rat anterior pituitary membranes. Recently, *Lewis and Williams* (25) reported that a single protein band in rat anterior pituitary membranes with slightly higher molecular weight was photoaffinity labeled by [^{125}I]Tyr11-SRIF.

Although the size of the SRIF receptor in GH3 and AtT-20 cells appears similar, charge differences between the proteins could significantly contribute to variations in their functional characteristics. However, analysis of the receptors covalently labeled with [^{125}I]CGP 23996 in GH3 and AtT-20 cell membranes by two-dimensional PAGE revealed that the receptors have similar size and pI values. Furthermore, the peptide maps of the SRIF receptors of both cell lines following protease digestion were similar. These studies suggest that major differences in structure do not exist between the SRIF receptor subtypes in AtT-20 and GH3 cells.

Pretreatment of AtT-20 cells with different SRIF analogues reduced both the equilibrium and covalent labeling of the SRIF receptors by [^{125}I]CGP 23996. Srikant and Heisler (26) have also shown that pretreatment of AtT-20 cells with SRIF decreases the equilibrium binding of [^{125}I]Tyr11-SRIF to membranes from these cells. In contrast, prolonged exposure of GH3 cells to Trp8-SRIF did not diminish the photoincorporation of [^{125}I]CGP 23996 into the SRIF receptor. Thus, despite the similarity in the structure of these receptors, they are differentially regulated.

The varying pharmacological characteristics of SRIF receptors in AtT-20 and GH3 cells could be due to subtle differences in the structure of the receptors which are not detected by the procedures employed in this study. Slight variations in the amino acid sequence could result in dramatic differences in the selectivity of the receptor for agonists. Differential processing of the SRIF receptor could also lead to small molecules being added to the receptor either in the AtT-20 or the GH3 cells. In fact, Susini *et al.* (27) have shown that the pancreatic SRIF receptor is a glycoprotein. Variations in the sugar composition or other post-translational modifications may exist between the SRIF receptor in AtT-20 and GH3 cells which could be responsible for the contrasting pharmacological characteristics of the receptor in the two cell lines. Elucidation of the post-translational processes, which induce the functional differences of these receptor subtypes, will be essential in understanding the mechanisms of action of SRIF and its prohormone in the

regulation of neuronal activity in brain and hormone secretion from endocrine and exocrine organs.

References

1. Epelbaum, J. Somatostatin in the central nervous system: physiological and pathological modifications. Prog. *Neurobiol.* **27**:63–100 (1986).
2. Srikant, C., and Y. Patel. Receptor binding of somatostatin 28 is tissue specific. *Nature (Lond.)* **294**:259–260 (1981).
3. Reubi, J., M. Perrin, J. Rivier, and W. Vale. High affinity binding sites for somatostatin 28 analog in rat brain. *Life Sci.* **28**:2191–2198 (1981).
4. Czernik, A., and B. Petrack. Somatostatin receptor binding in rat cerebral cortex, characterization using a non-reducible somatostatin analog. *J. Biol. Chem.* **258**:5525–5530 (1983).
5. Reubi, J., M. Perrin, J. Rivier, and W. Vale. Pituitary somatostatin receptors: dissociation at the pituitary level of receptor affinity and biological activity for selective somatostatin analogues. *Regul. Peptides* **4**:141–146 (1983).
6. Srikant, C., and Y. Patel. Somatostatin receptors on rat pancreatic acinar cells. *J. Biol. Chem.* **261**:7690–7696 (1986).
7. Sakamoto, C., I. Goldfine, and J. Williams. The somatostatin receptor on isolated pancreatic acinar cell plasma membranes. *J. Biol. Chem.* **259**:9623–9627 (1984).
8. Reubi, J. Evidence for two somatostatin-14 receptor types in rat brain cortex. *Neurosci. Lett.* **49**:259–263 (1984).
9. Tran, V., F. Beal, and J. Martin. Two types of somatostatin receptors differentiated by cyclic somatostatin analogues. *Science (Wash. D.C.)* **228**:492–495 (1985).
10. Brown, M., J. Rivier, and W. Vale. Somatostatin-28: selective actions on the pancreatic beta-cells and brain. *Endocrinology* **108**:2391–2393 (1981).
11. Mandarino, L., D. Stenner, W. Blanchard, S. Nissen, J. Gerich, N. Ling, P. Brazeau, P. Bohlem, F. Esch and R. Guillemin. Selective effects of somatostatin-14, -25, and -28 on *in vitro* insulin and glucagon secretion. *Nature (Lond.)* **291**:76–78, (1981).
12. Axelrod, J., and T. Reisine. Stress hormones: their interaction and regulation. *Science (Wash. D.C.)* **224**:452–459 (1984).
13. Schonbrunn, A., O. Rorstad, J. Westerdorf, and J. Martin. Somatostatin analogues: correlation between receptor binding affinity and biological activity in GH pituitary cells. *Endocrinology* **113**:1559–1567 (1983).
14. Reisine, T. Multiple mechanisms of somatostatin inhibition of adrenocorticotropin release from mouse anterior pituitary tumor cells. *Endocrinology* **116**:2259–2266 (1985).
15. Reisine, T., and S. Guild. Pertussis toxin blocks somatostatin inhibition of calcium mobilization and desensitizes somatostatin receptors. *J. Pharmacol. Exp. Ther.* **235**:551–557 (1985).
16. Tsien, R., T. Pozzan, and T. Rink. Calcium homeostasis in intact lymphocytes: cytoplasmic free calcium monitored with a new intracellularly trapped fluorescent indicator. *J. Cell Biol.* **94**:325–334 (1982).
17. Laemmli, U. Cleavage of structural proteins during the assembly of the head of bacteriophage T4. *Nature (Lond.)* **227**:680–685 (1970).
18. O'Farrell, P. High resolution two-dimensional electrophoresis of proteins. *J. Biol. Chem.* **250**:4007–4021 (1975).
19. Cleveland, D., S. Fischer, M. Kirschner, and U. Laemmli. Peptide mapping by limited proteolysis in sodium dodecyl sulfate and analysis by gel electrophoresis. *J. Biol. Chem.* **252**:1102–1106 (1977).
20. McGonigle, P., R. Huff, and P. Molinoff. A comprehensive method for the quantitative determination of dopamine receptor subtypes. *Ann. N. Y. Acad. Sci.* **430**:77–90 (1984).
21. Koch, B., L. Dorflinger, and A. Schonbrunn. Pertussis toxin blocks both cAMP-mediated and cAMP-independent actions of somatostatin. *J. Biol. Chem.* **260**:13138–13145 (1985).
22. Luini, A., D. Lewis, S. Guild, G. Sconfield, and F. Weight. Somtostatin, an inhibitor of ACTH secretion, decreases cytosolic free calcium and voltage regulated calcium current in a pituitary cell line. *J. Neurosci.* **6**:3128–3132 (1986).
23. Smith, M., G. Yamamoto, and W. Vale. Somatostatin desensitization in rat anterior pituitary cells. *Mol. Cell. Endocrinol.* **37**:311–318 (1984).
24. Marki, F., W. Bucher, and J. Richter. Multiple subcutaneous injections of somatostatin induce tachyphylaxis of the suppression of plasma insulin, but not glucagon, in the rat. *Regul. Peptides* **4**:333–339 (1982).
25. Lewis, L., and J. Williams. Structural characteristics of the somatostatin receptor in rat anterior pituitary membranes. *Endocrinology* **121**:486–492 (1987).
26. Srikant, C., and S. Heisler. Relationship between receptor binding and biopotency of somatostatin-14 and somatostatin-28 in mouse pituitary tumor cells. *Endocrinology* **117**:271–278 (1985).
27. Susini, C., A. Bailey, J. Szecowka, and J. Williams. Characterization of covalently cross-linked pancreatic somatostatin receptors. *J. Biol. Chem.* **261**:16738–16743 (1986).

Send reprint requests to: Dr. Terry Reisine, Department of Pharmacology, University of Pennsylvania School of Medicine, 36th and Hamilton Walk, Philadelphia, PA 19104.